J Stat Phys
DOI 10.1007/s10955-008-9610-3

Weakly Non-Ergodic Statistical Physics

A. Rebenshtok · E. Barkai

Received: 27 April 2008 / Accepted: 30 July 2008

Abstract For weakly non ergodic systems, the probability density function of a time average observable $\overline{\mathcal{O}}$ is $f_\alpha(\overline{\mathcal{O}}) = -\frac{1}{\pi}\lim_{\epsilon\to 0}\mathrm{Im}\frac{\sum_{j=1}^{L} p_j^{\mathrm{eq}}(\overline{\mathcal{O}}-\mathcal{O}_j+i\epsilon)^{\alpha-1}}{\sum_{j=1}^{L} p_j^{\mathrm{eq}}(\overline{\mathcal{O}}-\mathcal{O}_j+i\epsilon)^{\alpha}}$ where $\mathcal{O}_j$ is the value of the observable when the system is in state $j = 1, \ldots L$. p_j^{eq} is the probability that a member of an ensemble of systems occupies state j in equilibrium. For a particle undergoing a fractional diffusion process in a binding force field, with thermal detailed balance conditions, p_j^{eq} is Boltzmann's canonical probability. Within the unbiased sub-diffusive continuous time random walk model, the exponent $0 < \alpha < 1$ is the anomalous diffusion exponent $\langle x^2\rangle \sim t^\alpha$ found for free boundary conditions. When $\alpha \to 1$ ergodic statistical mechanics is recovered $\lim_{\alpha\to 1} f_\alpha(\overline{\mathcal{O}}) = \delta(\overline{\mathcal{O}} - \langle\mathcal{O}\rangle)$. We briefly discuss possible physical applications in single particle experiments.

Keywords Weak ergodicity breaking · Continuous time random walk · Fractional Fokker–Planck equation

1 Introduction

An ensemble of non-interacting one dimensional Brownian particles in the presence of a binding potential field $V(x)$ reach a thermal equilibrium described by Boltzmann's canonical law $p^{\mathrm{eq}}(x) = \exp[-V(x)/T]/Z$ where T is the temperature (units $k_b = 1$) and Z is the normalizing partition function. With this law we may calculate ensemble averages; for example $\langle x\rangle = \int_{-\infty}^{\infty} x p^{\mathrm{eq}}(x)\mathrm{d}x$. On the other hand, from the trajectory of a single particle $x(t)$ we may construct the time average $\overline{x} = \int_0^t x(t')\mathrm{d}t'/t$. For ergodic motion, the time and ensemble averages are identical in the limit of long measurement times $t \to \infty$. What is the Physical meaning of a long measurement time? Brownian motion in a finite interval is characterized by a finite relaxation time, the time scale on which particles reach thermal equilibrium. For the simplest case of Brownian motion between two reflecting walls, with a system

A. Rebenshtok · E. Barkai (✉)
Department of Physics, Bar Ilan University, Ramat-Gan 52900, Israel
e-mail: barkaie@mail.biu.ac.il

of size l, dimensional analysis gives a relaxation time of the order l^2/D, where D is the diffusion constant. A second time scale, the average time between jump events $\langle\tau\rangle$, is more microscopical. The latter is related to D with the Einstein relation [1] $D = \langle(\Delta x)^2\rangle/2\langle\tau\rangle$, where $\langle(\Delta x)^2\rangle$ is the variance of jump lengths. Ergodicity is almost trivial when the measurement time is much longer than these two time scales as in the case of a Brownian motion in a Harmonic field.

On the other hand, anomalous diffusion and transport are characterized in many cases by a diverging relaxation time and a diverging microscopical time scale $\langle\tau\rangle$. For example, unbiased sub-diffusion is characterized by a mean square displacement $\langle x^2\rangle \propto t^\alpha$ and $0 < \alpha < 1$. The reader immediately realizes that the diffusion constant is zero, in the sense that $\lim_{t\to\infty}\langle x^2\rangle/t = 0$. Hence the mentioned relaxation time l^2/D is infinite even when the system size l is finite. Indeed according to the continuous time random walk (CTRW) model [2–6], anomalous sub-diffusion is found when waiting times between jumps diverge $\langle\tau\rangle \to \infty$, which is related to the Scher-Montroll power law waiting time probability density function (PDF) $\psi(\tau) \propto \tau^{-(1+\alpha)}$ [2]. For such scale free anomalous diffusion, the relaxation time and the averaged sojourn time $\langle\tau\rangle$ are infinite, and ergodicity is broken weakly.

Strong ergodicity breaking is found when a system is divided into inaccessible regions of its phase space. Namely, a particle or a system starting in one region cannot explore all other regions due to some non-passable barrier (e.g. in the micro-canonical case regions refer to sections on the constant energy surface). Bouchaud [7] introduced the profound concept of weak ergodicity breaking in the context of glass dynamics, which in turn is related to infinite ergodic theory [8] investigated by Mathematicians using a dynamical approach. In weak ergodicity breaking, the phase space is not divided into inaccessible regions. Instead, due to the power law sticking times, the dynamics are non-stationary and non-ergodic.

Since the ergodic hypothesis is the pillar on which statistical mechanics is built, but at the same time also long tailed power law distributions of trapping times are very common in the description of Physical behaviors [2–6], it is natural to investigate the non-ergodic properties of systems whose stochastic dynamics are governed by such anomalous statistics. Previously, weak ergodicity breaking was investigated for the following phenomena: blinking quantum dots [9–12], Lévy walks [13], occupation time statistics of the CTRW model [14, 15], the fractional Fokker–Planck equation [16], deterministic one dimensional maps [17–19], numerical simulations of fractional transport in a washboard potential [20] and in vivo gene regulation by DNA-binding proteins [21]. Recently, a relation between statistics of weak ergodicity breaking and statistics of non-self averaging in models of quenched disorder was found [22]. Hence, it is timely to present a general statistical mechanical framework for weak-ergodicity breaking.

In this manuscript we investigate the distribution of time averaged observables for weak ergodicity breaking. We explore the relations between ensemble averages and fluctuations of time averages, and investigate the transition from the localization limit $\alpha \to 0$ to the usual ergodic behavior found for $\alpha \to 1$. Specific examples for the distribution of $\overline{x}$ for a particle undergoing a sub-diffusive CTRW in a potential $V(x)$ are worked out in detail. In the second part of the paper, we derive our main results using a generalized CTRW approach. We investigate models with a single waiting time PDF and more general models with several types of such PDFs. A brief summary of some of our results was recently published in [23].

The theory of weak-ergodicity breaking is mathematically related to the arcsine distribution [24–26], and to its extensions [27, 28]. Consider a normal Brownian motion with free boundary conditions in one dimension $\dot{x}(t) = \eta(t)$, where $\eta(t)$ is Gaussian white noise. The time t^+ spent by the particle in $x > 0$ is called an occupation time. The naive expectation is that the single particle will occupy $x > 0$ for half of the measurement time t, when the latter

is long. Instead, the PDF of the occupation fraction is

$$f\left(\frac{t^+}{t}\right) = \frac{1}{\pi\sqrt{(t^+/t)(1-t^+/t)}}. \tag{1}$$

This arcsine law is related to the well known PDF of first-passage times from x to the origin, for simple Brownian motion. The latter PDF decays $t^{-3/2}$ for long first-passage times [25], and the averaged return time is infinite. Roughly speaking, during the dynamics of the particle, it will usually occupy either the domain $x > 0$ or the domain $x < 0$ for a duration that is of the order of the measurement time. Thus the arcsine PDF (1) has a U shape. This behavior is found because the Brownian motion was assumed to be unbounded. If we add reflecting walls on $x = l/2$ and $x = -l/2$ the dynamics will be ergodic and in the long time limit the particle spends half of the time in $(0, l/2)$ and the other half in $(-l/2, 0)$. The theory of weak ergodicity breaking, presented in this manuscript, is mathematically related to the arcsine law and is based on Lévy statistics. A key point is that for certain models of anomalous diffusion, occupation times remain random even for finite systems [14, 22].

The organization of the current work will now be detailed. In Sect. 2, distribution of time averaged observables for weakly non-ergodic systems is presented using general arguments not specific to a model. Properties of this distribution are investigated in Sect. 3 and in Sect. 4 the example of the distribution of $\overline{x}$ for a particle undergoing fractional dynamics in a binding potential is worked out in detail. In Sect. 5, we derive our main result using a CTRW approach, thus further justifying assumptions made in Sect. 2. Numerical simulations of $\overline{x}$ obtained from the CTRW process are compared with analytical theory in Sect. 5.4.

2 Distribution of Time Averaged Observables

We consider a system with L states and label them with an index $j = 1, \ldots L$. A time average of a Physical observable $\mathcal{O}$ is made. If the system is in state j, the Physical observable attains the value $\mathcal{O}_j$. The time spent by the system in state j is t_j and is called a residence time or an occupation time. The time average of the Physical observable is

$$\overline{\mathcal{O}} = \frac{\sum_{j=1}^{L} t_j \mathcal{O}_j}{\sum_{j=1}^{L} t_j}, \tag{2}$$

and $\min\{\mathcal{O}_j\} \leq \overline{\mathcal{O}} \leq \max\{\mathcal{O}_j\}$. As mentioned in the introduction, many physical systems, in their stochastic or deterministic dynamics, are known to be characterized by power law sojourn times in the states of the system [2–6]. We assume that the occupation time t_j is a sum of many such sojourn times. If the state j is visited many times, and the sojourn times are independent identically distributed random variables, Lévy's limit theorem will describe the statistics of the residence times t_j in the limit of long measurement time. Hence we argue that the PDF of t_j is a one sided Lévy PDF $l_{\alpha, p_j^{\mathrm{eq}}}(t_j)$ whose Laplace transform is

$$\int_0^\infty l_{\alpha, p_j^{\mathrm{eq}}}(t_j) \exp(-u t_j) \mathrm{d}t_j = \exp\left(-p_j^{\mathrm{eq}} u^\alpha\right), \tag{3}$$

and $0 < \alpha \leq 1$.[1] Later we find that $p_j^{\rm eq}$ is the probability that a member of an ensemble of systems occupies state j in equilibrium. For the CTRW with thermal detailed balance conditions, $p_j^{\rm eq}$ is Boltzmann's probability of finding the system in state j, $p_j^{\rm eq} = \exp(-E_j/T)/Z$, as we will show later.

The following generating function [26] is a useful tool for our analysis

$$\hat{f}_\alpha(\xi) = \left\langle \frac{1}{1+\xi\overline{\mathcal{O}}} \right\rangle = \sum_{k=0}^{\infty} (-1)^k \langle \overline{\mathcal{O}}^k \rangle \xi^k. \tag{4}$$

Our main aim is to find the PDF of the time averaged observable

$$f_\alpha\left(\overline{\mathcal{O}}\right) = \left\langle \delta\left(\overline{\mathcal{O}} - \frac{\sum_{j=1}^L \mathcal{O}_j t_j}{\sum_{j=1}^L t_j}\right)\right\rangle = -\frac{1}{\pi}\lim_{\epsilon\to 0}{\rm Im}\left\langle \frac{1}{\overline{\mathcal{O}} + i\epsilon - \frac{\sum_{j=1}^L \mathcal{O}_j t_j}{\sum_{j=1}^L t_j}}\right\rangle$$

$$= -\frac{1}{\pi}\lim_{\epsilon\to 0}{\rm Im}\frac{1}{\overline{\mathcal{O}}+i\epsilon}\left\langle \frac{1}{1-\frac{1}{\overline{\mathcal{O}}+i\epsilon}\frac{\sum_{j=1}^L \mathcal{O}_j t_j}{\sum_{j=1}^L t_j}}\right\rangle, \tag{5}$$

using (4)

$$f_\alpha\left(\overline{\mathcal{O}}\right) = -\frac{1}{\pi}\lim_{\epsilon\to 0}{\rm Im}\frac{1}{\overline{\mathcal{O}}+i\epsilon}\hat{f}_\alpha\left(-\frac{1}{\overline{\mathcal{O}}+i\epsilon}\right). \tag{6}$$

We now find the generating function (4) and invert it using (6) to obtain $f_\alpha(\overline{\mathcal{O}})$.

The generating function is rewritten

$$\hat{f}_\alpha(\xi) = \left\langle \int_0^\infty {\rm d}s e^{-\left(1+\xi\frac{\sum_{j=1}^L \mathcal{O}_j t_j}{\sum_{j=1}^L t_j}\right)s}\right\rangle$$

$$= \int_0^\infty {\rm d}s \int_0^\infty {\rm d}t \int_0^\infty {\rm d}t_1 l_{\alpha,p_1^{\rm eq}}(t_1)\cdots\int_0^\infty {\rm d}t_L l_{\alpha,p_L^{\rm eq}}(t_L)$$

$$\times\,\delta\left(t - \sum_{j=1}^L t_j\right) e^{-\left(1+\xi\frac{\sum_{j=1}^L \mathcal{O}_j t_j}{t}\right)s}. \tag{7}$$

Using a well known presentation for the delta function in (7)

$$\delta\left(t - \sum_{j=1}^L t_j\right) = \frac{1}{2\pi}\int_{-\infty}^\infty {\rm d}k e^{ik\left(t-\sum_{j=1}^L t_j\right)}, \tag{8}$$

changing variables $kt = \tilde{k}$ and using (3) we find

$$\hat{f}_\alpha(\xi) = \int_0^\infty {\rm d}t t^{-1}\int_{-\infty}^\infty \frac{{\rm d}\tilde{k}}{2\pi}\int_0^\infty {\rm d}s \exp\left[i\tilde{k} - s - \sum_{j=1}^L p_j^{\rm eq}\frac{\left(i\tilde{k}+\mathcal{O}_j\xi s\right)^\alpha}{t^\alpha}\right]. \tag{9}$$

[1] See [5, 24, 29, 30] and Ref. therein for properties of one sided Lévy stable laws. Note that the Laplace variable u in (3) is dimensionless. We may use $\exp(-Bp_j^{\rm eq}u^\alpha)$ in (3) with $B > 0$ however our final result (13) does not depend on it thus we take $B = 1$.

We again change variables $k = \tilde{k}/t$ and $\tilde{s} = s/t$ and obtain

$$\hat{f}_\alpha(\xi) = \int_0^\infty \mathrm{d}t \int_{-\infty}^\infty \frac{\mathrm{d}k}{2\pi} \int_0^\infty \mathrm{d}\tilde{s}\, t \exp\left[ikt - \tilde{s}t - \sum_{j=1}^{L} p_j^{\mathrm{eq}} \left(ik + \mathcal{O}_j \xi \tilde{s}\right)^\alpha \right]. \tag{10}$$

This equation is rewritten using a simple trick

$$\hat{f}_\alpha(\xi) = \int_0^\infty \mathrm{d}t \int_{-\infty}^\infty \frac{\mathrm{d}k}{2\pi} \int_0^\infty \mathrm{d}\tilde{s} \left\{ -\frac{\mathrm{d}}{\mathrm{d}\tilde{s}} \exp\left[ikt - \tilde{s}t - \sum_{j=1}^{L} p_j^{\mathrm{eq}} \left(ik + \mathcal{O}_j \xi \tilde{s}\right)^\alpha \right] \right.$$
$$\left. - \alpha \sum_{j=1}^{L} p_j^{\mathrm{eq}} \left(ik + \mathcal{O}_j \xi \tilde{s}\right)^{\alpha-1} \mathcal{O}_j \xi \exp\left[(ik - \tilde{s})\, t - \sum_{j=1}^{L} p_j^{\mathrm{eq}} \left(ik + \mathcal{O}_j \xi \tilde{s}\right)^\alpha \right] \right\}. \tag{11}$$

Integration over t gives a simple pole $1/(ik - \tilde{s})$, using Cauchy integral formula to integrate over k, and then solving two trivial integrals yields

$$\hat{f}_\alpha(\xi) = \frac{\sum_{j=1}^{L} p_j^{\mathrm{eq}} \left(1 + \mathcal{O}_j \xi\right)^{\alpha-1}}{\sum_{j=1}^{L} p_j^{\mathrm{eq}} \left(1 + \mathcal{O}_j \xi\right)^{\alpha}}. \tag{12}$$

Inverting (12) using (6) we find

$$f_\alpha\left(\overline{\mathcal{O}}\right) = -\frac{1}{\pi} \lim_{\epsilon \to 0} \mathrm{Im} \frac{\sum_{j=1}^{L} p_j^{\mathrm{eq}} \left(\overline{\mathcal{O}} - \mathcal{O}_j + i\epsilon\right)^{\alpha-1}}{\sum_{j=1}^{L} p_j^{\mathrm{eq}} \left(\overline{\mathcal{O}} - \mathcal{O}_j + i\epsilon\right)^{\alpha}}. \tag{13}$$

This is a very general formula for the distribution of time averaged observables for weakly non-ergodic systems. As we show later, within the CTRW model, α is the anomalous diffusion exponent. For $0 < \alpha < 1$ we use $\lim_{\epsilon \to 0} (\overline{\mathcal{O}} - \mathcal{O}_j + i\epsilon)^\alpha = |\overline{\mathcal{O}} - \mathcal{O}_j|^\alpha e^{i\phi_j \alpha}$ where $\phi_j = \begin{pmatrix} \pi \text{ if } \overline{\mathcal{O}} < \mathcal{O}_j \\ 0 \text{ if } \overline{\mathcal{O}} \geq \mathcal{O}_j \end{pmatrix}$ and (13) becomes

$$f_\alpha\left(\overline{\mathcal{O}}\right) = \frac{\sin \pi\alpha}{\pi} \frac{I_{\alpha-1}^{<}\left(\overline{\mathcal{O}}\right) I_\alpha^{\geq}\left(\overline{\mathcal{O}}\right) + I_{\alpha-1}^{\geq}\left(\overline{\mathcal{O}}\right) I_\alpha^{<}\left(\overline{\mathcal{O}}\right)}{\left[I_\alpha^{\geq}\left(\overline{\mathcal{O}}\right)\right]^2 + \left[I_\alpha^{<}\left(\overline{\mathcal{O}}\right)\right]^2 + 2 I_\alpha^{\geq}\left(\overline{\mathcal{O}}\right) I_\alpha^{<}\left(\overline{\mathcal{O}}\right) \cos \pi\alpha}, \tag{14}$$

with

$$I_\alpha^{<}\left(\overline{\mathcal{O}}\right) = \sum_{\overline{\mathcal{O}} < \mathcal{O}_j} p_j^{\mathrm{eq}} |\overline{\mathcal{O}} - \mathcal{O}_j|^\alpha \tag{15}$$

and

$$I_\alpha^{\geq}\left(\overline{\mathcal{O}}\right) = \sum_{\overline{\mathcal{O}} \geq \mathcal{O}_j} p_j^{\mathrm{eq}} |\overline{\mathcal{O}} - \mathcal{O}_j|^\alpha. \tag{16}$$

Notice the L divergences of $f_\alpha(\overline{\mathcal{O}})$ when $\overline{\mathcal{O}} = \mathcal{O}_j$ due to the $I_{\alpha-1}^{\geq}(\mathcal{O})$ term in the numerator of (14). This behavior is caused by long sticking times in a state of the system, on a time scale that is of the order of the measurement time.

3 Statistics of Weak Ergodicity Breaking

In this section we investigate properties of (12), (13).

3.1 Limits $\alpha \to 0$ and $\alpha \to 1$

In the limit $\alpha \to 1$ we recover usual ergodic behavior. From (13)

$$f_1\left(\overline{\mathcal{O}}\right) = -\frac{1}{\pi}\lim_{\epsilon\to 0}\mathrm{Im}\frac{\sum_{j=1}^{L} p_j^{\mathrm{eq}}}{\sum_{j=1}^{L} p_j^{\mathrm{eq}}\left(\overline{\mathcal{O}} - \mathcal{O}_j + i\epsilon\right)}. \tag{17}$$

Using the normalization condition $\sum_{j=1}^{L} p_j^{\mathrm{eq}} = 1$ and the ensemble average

$$\langle \mathcal{O}\rangle = \sum_{j=1}^{L} p_j^{\mathrm{eq}}\mathcal{O}_j \tag{18}$$

we have ergodic behavior

$$f_1\left(\overline{\mathcal{O}}\right) = \delta(\overline{\mathcal{O}} - \langle \mathcal{O}\rangle) \tag{19}$$

in the sense that the ensemble average is equal to the time average. Note that already (3) in the limit $\alpha \to 1$ indicates ergodicity since the residence time is not a fluctuating quantity (i.e. the one sided Lévy PDF is a delta function when $\alpha = 1$). In the opposite limit of $\alpha \to 0$ we find

$$\lim_{\alpha\to 0} f_\alpha\left(\overline{\mathcal{O}}\right) = -\frac{1}{\pi}\lim_{\epsilon\to 0}\mathrm{Im}\sum_{j=1}^{L} p_j^{\mathrm{eq}}\left(\overline{\mathcal{O}} - \mathcal{O}_j + i\epsilon\right)^{-1} \tag{20}$$

hence

$$\lim_{\alpha\to 0} f_\alpha\left(\overline{\mathcal{O}}\right) = \sum_{j=1}^{L} p_j^{\mathrm{eq}}\delta\left(\overline{\mathcal{O}} - \mathcal{O}_j\right). \tag{21}$$

This describes a localization behavior where the system is stuck in one of the states for the whole duration of the observation time, which is the expected behavior when $\alpha \to 0$.

3.2 Lamperti Statistics of the Occupation Fraction

Let the Physical observable be $\mathcal{O}_j = 1$ when $j = 1, \ldots, \bar{l}$ where $\bar{l} \le L$, otherwise $\mathcal{O}_j = 0$. Hence the time average in this case is the occupation fraction

$$\overline{\mathcal{O}} = \frac{\sum_{j=1}^{\bar{l}} t_j}{\sum_{j=1}^{L} t_j} \tag{22}$$

which is the fraction of time spent by the system in the observation domain $j = 1, \ldots, \bar{l}$. Clearly $0 \le \overline{\mathcal{O}} \le 1$ in this case. Using (13) a straight forward calculation gives

$$f_\alpha\left(\overline{\mathcal{O}}\right) = \frac{1}{\pi}\frac{\mathcal{R}\left[\left(1-\overline{\mathcal{O}}\right)\overline{\mathcal{O}}\right]^{\alpha-1}\sin\pi\alpha}{\mathcal{R}^2\left(1-\overline{\mathcal{O}}\right)^{2\alpha} + \overline{\mathcal{O}}^{2\alpha} + 2\mathcal{R}\left[\left(1-\overline{\mathcal{O}}\right)\overline{\mathcal{O}}\right]^{\alpha}\cos\pi\alpha}. \tag{23}$$

This is the Lamperti PDF [27] which is a natural generalization of the arcsine distribution [the case $\alpha = 1/2$, $\mathcal{R} = 1$ (1)]. The PDF (23) has found several applications in non-ergodic systems mentioned in the introduction [10, 14, 17–19, 21] and recently for the non-self averaging properties of the quenched trap model [22]. The parameter $\mathcal{R}$ in (23) is called the asymmetry parameter and is given by

$$\mathcal{R} = \frac{p^{\rm eq}_{1,\bar{l}}}{1 - p^{\rm eq}_{1,\bar{l}}}, \tag{24}$$

where $p^{\rm eq}_{1,\bar{l}} = \sum_{j=1}^{\bar{l}} p^{\rm eq}_j$ is the probability to be in the observation domain. Since the observable attains two values $\mathcal{O}_j = 1$ or $\mathcal{O}_j = 0$, the PDF (23) has two divergences on $\overline{\mathcal{O}} = 1$ and $\overline{\mathcal{O}} = 0$, which is a special case of the more general rule discussed after (16).

3.3 Low Order Moments of Time Averaged Observables

From the moment generating function $\hat{f}_\alpha(\xi)$, we can obtain moments of the time averages $\overline{\mathcal{O}}$:

$$\langle \overline{\mathcal{O}}^n \rangle = (-1)^n \frac{1}{n!} \frac{\partial^n}{\partial \xi^n} \hat{f}_\alpha(\xi)|_{\xi=0}. \tag{25}$$

Using (12) we find

$$\langle \overline{\mathcal{O}} \rangle = \sum_{j=1}^{L} p^{\rm eq}_j \mathcal{O}_j. \tag{26}$$

The average $\langle \ldots \rangle$ is over an ensemble of realizations. If the ensemble reaches an equilibrium then obviously $\langle \overline{\mathcal{O}} \rangle = \langle \mathcal{O} \rangle$ which is time independent. Hence the $p^{\rm eq}_j$s in (26) are the probabilities that a member of an ensemble of systems occupies state j when the ensemble reaches an equilibrium. This justifies our original assumption that the $p^{\rm eq}_j$s in (3) are population fractions. Namely, the $p^{\rm eq}_j$s can be in principle measured by letting many independent systems (or many non-interacting particles) evolve. Then in the long time limit $p^{\rm eq}_j$ is the number of systems in state j over the total number of systems when the latter is large. Using (12), (25), the fluctuations are given by

$$\langle \overline{\mathcal{O}}^2 \rangle - \langle \overline{\mathcal{O}} \rangle^2 = (1 - \alpha) \left(\langle \mathcal{O}^2 \rangle - \langle \mathcal{O} \rangle^2 \right), \tag{27}$$

where $\langle \mathcal{O}^2 \rangle = \sum_{j=1}^{L} p^{\rm eq}_j (\mathcal{O}_j)^2$. Equation (27) gives a simple relation between fluctuations of time averages and fluctuations of ensemble averages. Once again, when $\alpha = 1$ the fluctuations of the time average (27) vanish, indicating ergodic behavior. Relations between cumulants of time average observables and cumulants of ensemble averages are found in a similar way. For the third cumulant

$$\begin{aligned} C_3(\overline{\mathcal{O}}) &= \langle \overline{\mathcal{O}}^3 \rangle - 3\langle \overline{\mathcal{O}}^2 \rangle \langle \overline{\mathcal{O}} \rangle + 2\langle \overline{\mathcal{O}} \rangle^3 = \frac{1}{2}(2-\alpha)(1-\alpha) \left(\langle \mathcal{O}^3 \rangle - 3\langle \mathcal{O}^2 \rangle \langle \mathcal{O} \rangle + 2\langle \mathcal{O} \rangle^3 \right) \\ &= \frac{1}{2}(2-\alpha)(1-\alpha) C_3(\mathcal{O}) \end{aligned} \tag{28}$$

and the fourth cumulant

$$C_4(\overline{\mathcal{O}}) = \langle \overline{\mathcal{O}}^4 \rangle - 4\langle \overline{\mathcal{O}}^3 \rangle \langle \overline{\mathcal{O}} \rangle - 3\langle \overline{\mathcal{O}}^2 \rangle^2 + 12\langle \overline{\mathcal{O}}^2 \rangle \langle \overline{\mathcal{O}} \rangle^2 - 6\langle \overline{\mathcal{O}} \rangle^4$$

$$= (1-\alpha)\Bigg(\frac{(3-\alpha)(2-\alpha)}{6}\left(\langle\mathcal{O}^4\rangle - 4\langle\mathcal{O}^3\rangle\langle\mathcal{O}\rangle\right) + \left(6-6\alpha+\alpha^2\right)\left(\langle\mathcal{O}\rangle^2\left(2\langle\mathcal{O}^2\rangle - \langle\mathcal{O}\rangle^2\right)\right) - \frac{1}{2}(6-\alpha)(1-\alpha)\langle\mathcal{O}^2\rangle^2\Bigg). \quad (29)$$

Low order moments of time averaged observables can be expressed using the cumulants (27), (28), (29). The results remain as cumbersome as the expressions in (28), (29). When the odd moments of the ensemble average equal zero $\langle\mathcal{O}^{2n-1}\rangle = 0\ n = 1, 2, \ldots$, corresponding to examples we investigate in Sect. 4, the expressions for moments are simpler. Odd moments of the time average observable are equal to zero, as expected. The second moment is $\langle\overline{\mathcal{O}}^2\rangle = (1-\alpha)\langle\mathcal{O}^2\rangle$ and the fourth moment

$$\langle\overline{\mathcal{O}}^4\rangle = \frac{(3-\alpha)(2-\alpha)(1-\alpha)}{6}\langle\mathcal{O}^4\rangle + \frac{\alpha(1-\alpha)^2}{2}\langle\mathcal{O}^2\rangle^2. \quad (30)$$

3.4 Correlations Between Occupation Fractions $\langle\overline{p}_l\overline{p}_k\rangle$

The correlations between the occupation fractions $\overline{p}_l = t_l/t$ and $\overline{p}_k = t_k/t$ where $t = \sum_{j=1}^{L} t_j$ are now briefly investigated. We use the L dimensional vector $\vec{\xi} = \{\xi_1, \xi_2, \ldots \xi_L\}$ and the L dimensional generating function

$$\hat{g}_\alpha(\vec{\xi}) = \left\langle \frac{1}{1+\sum_{j=1}^{L}\xi_j\overline{p}_j}\right\rangle. \quad (31)$$

Related multidimensional arcsine distribution of occupation fractions were investigated in [28]. Using the substitution $\xi\mathcal{O}_j \to \xi_j$, in (4) it is easy to see using (12):

$$\hat{g}_\alpha(\vec{\xi}) = \frac{\sum_{j=1}^{L} p_j^{\rm eq}(1+\xi_j)^{\alpha-1}}{\sum_{j=1}^{L} p_j^{\rm eq}(1+\xi_j)^{\alpha}}. \quad (32)$$

This multidimensional generating function yields

$$\langle\overline{p}_j\rangle = -\frac{\partial}{\partial\xi_j}\hat{g}_\alpha(\vec{\xi})|_{\vec{\xi}=0} = p_j^{\rm eq} \quad (33)$$

and similarly, by taking the second order derivative of $\hat{g}_\alpha(\vec{\xi})$ with respect to ξ_j

$$\langle\overline{p}_j^2\rangle - \langle\overline{p}_j\rangle^2 = (1-\alpha)p_j^{\rm eq}\left(1-p_j^{\rm eq}\right). \quad (34)$$

Identical results can be obtained using the Lamperti PDF (23). It is more interesting to notice the correlations between occupation fractions, for example

$$\langle\overline{p}_l\overline{p}_k\rangle = \frac{1}{2}\frac{\partial}{\partial\xi_k}\frac{\partial}{\partial\xi_l}\hat{g}_\alpha(\vec{\xi})|_{\vec{\xi}=0} \quad (35)$$

for $l \neq k$. Using (32)

$$\langle\overline{p}_l\overline{p}_k\rangle = \alpha p_l^{\rm eq}p_k^{\rm eq}. \quad (36)$$

We see that when $\alpha \to 1$ the occupation fractions are uncorrelated since $\langle\overline{p}_l\overline{p}_k\rangle - \langle\overline{p}_l\rangle\langle\overline{p}_k\rangle = 0$. When $\alpha \to 0$ the system occupies one state for practically the whole duration of the measurement, hence either $\overline{p}_l \simeq 1$ and then obviously $\overline{p}_k \simeq 0$ or the opposite

situation is found, or both occupation fractions are zero (if $L > 2$). In any case, clearly the product $\overline{p}_l \overline{p}_k$ is zero when $\alpha \to 0$ and $l \neq k$ as we have indeed found in (36).

4 Distribution of $\overline{x}$

We now consider a particle undergoing stochastic fractional dynamics in a binding field. The fractional Fokker–Planck equation [31, 32] describes anomalous sub-diffusion and relaxation close to thermal equilibrium using fractional calculus,

$$\frac{\partial^\alpha p(x,t)}{\partial t^\alpha} = D_\alpha \left[\frac{\partial^2}{\partial x^2} - \frac{\partial}{\partial x} \frac{F(x)}{T} \right] p(x,t), \tag{37}$$

where D_α is the fractional diffusion coefficient, and $F(x) = -\partial V(x)/\partial x$ is the force. Equation (37) reduces to the usual Fokker–Planck equation when $\alpha = 1$. The fractional Fokker–Planck equation was derived from the sub-diffusive continuous time random walk [32] which is the stochastic process we have in mind. In the absence of the force field and for free boundary conditions $\langle x^2 \rangle = 2D_\alpha t^\alpha$. An important property of the fractional Fokker–Planck equation is that in the long time limit, Boltzmann equilibrium is obtained [31]

$$p^{\rm eq}(x) = \frac{\exp\left[-\frac{V(x)}{T}\right]}{Z} \tag{38}$$

provided that the force is binding. Recently, numerical methods that provide the sample paths of the fractional Fokker–Planck equation were investigated in detail [20, 33–36]. Such paths or the corresponding CTRW trajectories yield non ergodic behaviors [14]. For example, in [16], the Lamperti PDF (23) of the occupation fraction was obtained from the fractional equation (37). However distributions of time averages of physical observables have yet to be considered in detail.

We investigate the time average of the observable $\mathcal{O} = x$ with $-\infty < x < \infty$ so we are dealing with a continuum situation. Taking the continuum limit of (13) we find

$$f_\alpha(\overline{x}) = -\frac{1}{\pi} \lim_{\epsilon \to 0} {\rm Im} \frac{\int_{-\infty}^{\infty} {\rm d}x p^{\rm eq}(x) (\overline{x} - x + i\epsilon)^{\alpha-1}}{\int_{-\infty}^{\infty} {\rm d}x p^{\rm eq}(x) (\overline{x} - x + i\epsilon)^{\alpha}}, \tag{39}$$

which for $0 < \alpha < 1$ is rewritten as

$$f_\alpha(\overline{x}) = \frac{\sin \pi\alpha}{\pi} \frac{I^<_{\alpha-1}(\overline{x}) I^>_\alpha(\overline{x}) + I^>_{\alpha-1}(\overline{x}) I^<_\alpha(\overline{x})}{\left[I^>_\alpha(\overline{x})\right]^2 + \left[I^<_\alpha(\overline{x})\right]^2 + 2\cos\pi\alpha I^>_\alpha(\overline{x}) I^<_\alpha(\overline{x})}, \tag{40}$$

where

$$I^<_\alpha(\overline{x}) = \int_{\overline{x}}^{\infty} {\rm d}x p^{\rm eq}(x) |x - \overline{x}|^\alpha \tag{41}$$

and

$$I^>_\alpha(\overline{x}) = \int_{-\infty}^{\overline{x}} {\rm d}x p^{\rm eq}(x) |\overline{x} - x|^\alpha \tag{42}$$

and similarly for $I^<_{\alpha-1}(\overline{x})$ and $I^>_{\alpha-1}(\overline{x})$. When $\alpha \to 0$ we have $\lim_{\alpha\to 0} f_\alpha(\overline{x}) = p^{\rm eq}(\overline{x})$, which is the continuum limit of (21). In the ergodic limit $\alpha \to 1$ we find $f_1(\overline{x}) = \delta(\overline{x} - \langle x \rangle)$.

4.1 Free Particle

As an example, consider a particle in a domain $-l/2 < x < l/2$ undergoing an unbiased fractional random walk with reflecting walls. This is a free particle in the sense that no external field is acting on it. The time average of the particle's position $\overline{x}$ is considered, and obviously for this case $p^{\rm eq}(x) = 1/l$ for $-l/2 < x < l/2$. Using (40) we find the PDF of $\overline{x}$

$$f_\alpha(\overline{x}) = \frac{1}{l} \frac{N_\alpha \left(\frac{1}{4} - \frac{\overline{x}^2}{l^2}\right)^\alpha}{\left|\frac{1}{2} - \frac{\overline{x}}{l}\right|^{2(1+\alpha)} + \left|\frac{1}{2} + \frac{\overline{x}}{l}\right|^{2(1+\alpha)} + 2\left|\frac{1}{4} - \left(\frac{\overline{x}}{l}\right)^2\right|^{1+\alpha} \cos \pi\alpha}, \tag{43}$$

where $N_\alpha = (1+\alpha)\sin\pi\alpha/(\pi\alpha)$. When $\alpha \to 1$ we have ergodic behavior $f_\alpha(\overline{x}) = \delta(\overline{x})$ since $\langle x \rangle = 0$. However, in the opposite limit, $f_{\alpha\to 0}(\overline{x}) = 1/l$ for $|\overline{x}| < l/2$ which is the uniform distribution, reflecting the mentioned localization of the particle in space when $\alpha \to 0$.

4.2 Harmonic Oscillator

We consider the time average $\overline{x}$ of a particle in a Harmonic force field $V(x)/T = x^2$ so that $p^{\rm eq}(x) = \exp(-x^2)/\sqrt{\pi}$ and $\langle x \rangle = 0$. Using Mathematica, the integrals (41), (42) can be calculated explicitly and expressed in terms of tabulated confluent Hypergeometric functions. In Fig. 1 the PDF of $\overline{x}$ (40) is presented, and a transition from a narrow distribution when $\alpha \to 1$ to a Gaussian distribution when $\alpha \to 0$, $\lim_{\alpha\to 0} f_\alpha(\overline{x}) = p^{\rm eq}(\overline{x})$ is found. Using (40) it is easy to show that $\langle \overline{x} \rangle = 0$, $\langle \overline{x}^2 \rangle = (1-\alpha)\langle x^2 \rangle$ with $\langle x^2 \rangle = 1/2$ for $p^{\rm eq}(x)$ under consideration, and $\langle \overline{x}^4 \rangle = (1-\alpha)(3-2\alpha)\langle x^2 \rangle^2$. Only when $\alpha \to 0$ we have Gaussian statistics with $\langle \overline{x}^4 \rangle = 3\langle \overline{x}^2 \rangle^2$. The PDF $f_\alpha(\overline{x})$ at its maximum on $\overline{x} = 0$ is

$$f_\alpha(\overline{x} = 0) = \frac{\Gamma(\frac{\alpha}{2}) \tan(\frac{\pi\alpha}{2})}{\Gamma(\frac{1+\alpha}{2})\pi}, \tag{44}$$

which is equal to $p^{\rm eq}(x = 0) = 1/\sqrt{\pi}$ when $\alpha \to 0$ and diverges when $\alpha \to 1$ as expected from an ergodic behavior. For the Harmonic oscillator and the Free particles the maximum of $f_\alpha(\overline{x})$ is found on the ensemble average $\langle x \rangle = 0$, so the most likely result for $\overline{x}$ is $\langle x \rangle$. In

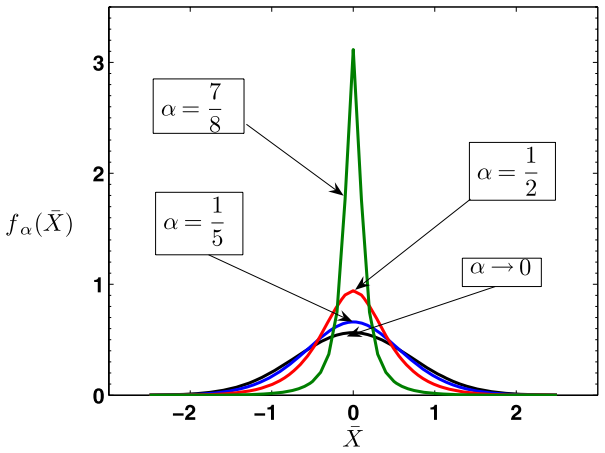

Fig. 1 The PDF of $\overline{x}$ for a particle in a Harmonic force field (40). We find a transition between an ergodic behavior: a delta distribution of $\overline{x}$ when $\alpha \to 1$, to the localization limit where the distribution of $\overline{x}$ is Gaussian when $\alpha \to 0$

the next subsection we consider a case where a minimum of $f_\alpha(\overline{x})$ is found on the ensemble average.

4.3 Double Well Potential

An interesting case is the symmetric double well potential $V(x)/T = (x^4/4 - x^2/2)/T$ therefore $\langle x \rangle = 0$. When the temperature $T \to 0$, $p^{\rm eq}(x)$ has two peaks centered on the two local minima of the double well potential. In this low temperature case and in the limit $\alpha \to 0$, we expect to find the particle either in the left well or in the right well for a time scale comparable to the measurement time. Thus when $T \to 0$ and $\alpha \to 0$ the PDF of the time average $\overline{x}$, $f_\alpha(\overline{x})$ is a sum of two delta functions since either $\overline{x} = 1$ or $\overline{x} = -1$. When $\alpha \to 1$, we expect an ergodic behavior, and then PDF $f_1(\overline{x}) = \delta(\overline{x})$, since $\langle x \rangle = 0$. So for low temperatures we expect a transition in the behavior of $f_\alpha(\overline{x})$ from a bimodal shape when $\alpha \to 0$ to a PDF with a single peak centered on zero when $\alpha \to 1$. Hence we will have a critical value α_c. For $\alpha < \alpha_c$ the shape of $f_\alpha(\overline{x})$ is bimodal with a minimum on $\overline{x} = 0$, while for $\alpha > \alpha_c$ a maximum on $\overline{x} = 0$ is found. These low temperature behaviors are shown in Fig. 2. For high temperatures (compared with the barrier height) the bimodal solution of $p^{\rm eq}(x)$ turns into a flatter shape. Since $\lim_{\alpha\to 0} f_\alpha(\overline{x}) = p^{\rm eq}(\overline{x})$, we will not observe the bimodal shape of $\lim_{\alpha\to 0} f_\alpha(\overline{x})$ when $T \to \infty$. Such high temperature behavior is shown in Fig. 3.

Investigating the extremum of $p^{\rm eq}(x)$ on $x = 0$ it is easy to show that α_c is finite for any finite temperature and $\alpha_c \to 0$ when $T \to \infty$. For $T = 0$ we have only two states in the system, either $x = -1$ or $x = 1$ corresponding to two minima of the double well potential. The analysis is then very similar to the two state ballistic Lévy walk model [10, 37]. Clearly $\overline{x}$ is the residence time in state $x = 1$ minus the residence time in state $x = -1$ divided by the measurement time t. Since the sum of these two residence times is the measurement time we can use the Lamperti distribution (23) to predict the distribution of $\overline{x}$. So when $T \to 0$

$$\lim_{T\to 0} f_\alpha(\overline{x}) = \frac{2\sin\pi\alpha}{\pi} \frac{\left(1-\overline{x}^2\right)^{\alpha-1}}{(1+\overline{x})^{2\alpha} + (1-\overline{x})^{2\alpha} + 2\left(1-\overline{x}^2\right)^{\alpha}\cos\pi\alpha}, \tag{45}$$

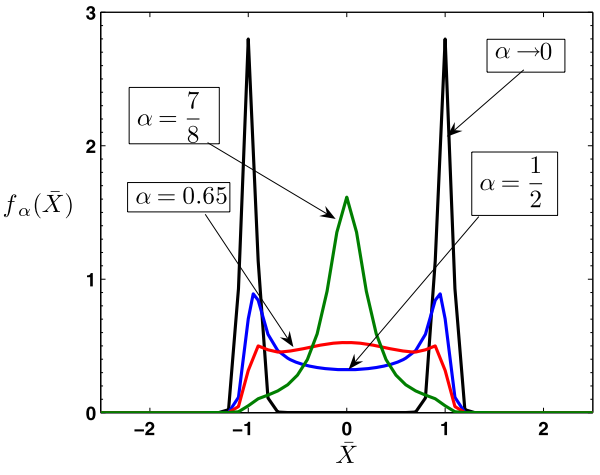

Fig. 2 The PDF of $\overline{x}$ for a particle in the double well potential with $T = 0.01$. A transition between a bimodal behavior when $\alpha < \alpha_c$ to a PDF with a peak on $\overline{x} = 0$ when $\alpha > \alpha_c$ is observed ($\alpha_c \simeq 0.59$ for this case). In the ergodic limit $\alpha \to 1$ $f_\alpha(\overline{x})$ is a delta function centered on the ensemble average $\langle x \rangle = 0$. In the localization limit $\alpha \to 0$ $f_\alpha(\overline{x})$ is equal to the population density $p^{\rm eq}(\overline{x})$

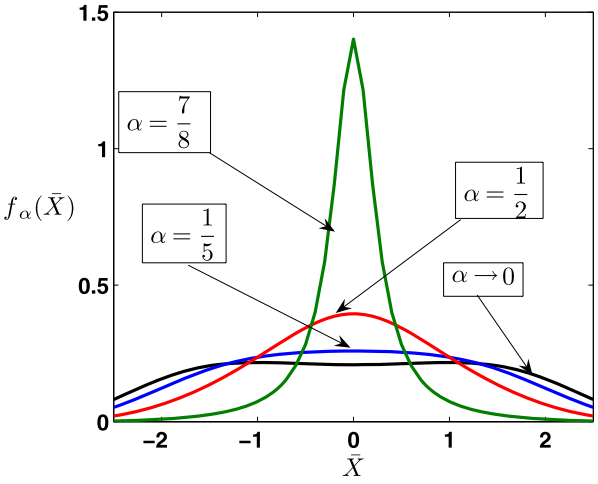

Fig. 3 The same as Fig. 2 however now $T = 7$. The bimodal shape presented in Fig. 2 is smoothed and we barely observe bimodal behavior, since the equilibrium density $p^{\rm eq}(x)$ is not centered around the two minima of the double well potential, when the temperature is high

which was found already in [26, 38]. We find that $\alpha_c = 0.59461\ldots$ when $T \to 0$. The behavior of α_c versus temperature is shown in Fig. 4 and the transition between the low and high temperature cases is presented.

4.4 Possible Physical Applications

It is interesting to verify experimentally our theoretical predictions and here we discuss three examples. Generally, systems with CTRW type of dynamics are natural candidates for the investigation of weak ergodicity breaking, provided that information of single particle dynamics can be recorded.

Sub-diffusion $\langle x^2 \rangle \sim t^\alpha$ *of a bead in a polymer network* was measured by Wong et al. [39]. The measured [39] exponent α depends on the ratio of the size of the bead and the linear size of the mesh of the network l (roughly a μm). We suggest to add an external binding field, for example an harmonic trap. The time averages of a single particle coordinate can then be measured, and according to our theory its distribution is given by (13). Such measurement can provide insight into the nature of disorder, for example whether it is quenched or annealed [22].

Messenger RNA molecules inside live E. coli cells exhibit anomalous diffusion $\langle x^2 \rangle \sim t^\alpha$ and $\alpha = 3/4$ [40]. Due to the finite size of the cell the motion is bounded. It would be interesting to investigate time averages of the position of the single molecule, or occupation time statistics, to investigate deviations from ergodicity. Our theory gives a prediction for the distribution of these observables, which can be tested experimentally.

Blinking quantum dots exhibit ergodicity breaking which is already measured in experiments [9, 11, 12]. So far a simple two state picture of the quantum dots was used, either the dot is on and it emits many photons, or it is off [10]. Then ergodicity breaking of the time averaged fluorescence intensity is similar to the time average of the particle's position in the double well potential in the limit of $T \to 0$, in the latter case either the particle is in the left well or in the right well. More careful analysis reveals that some dots deviate from a simple two state process [12]. Then our more general theory can be used in principle to predict distribution of time averaged intensity beyond the existing two state approach.

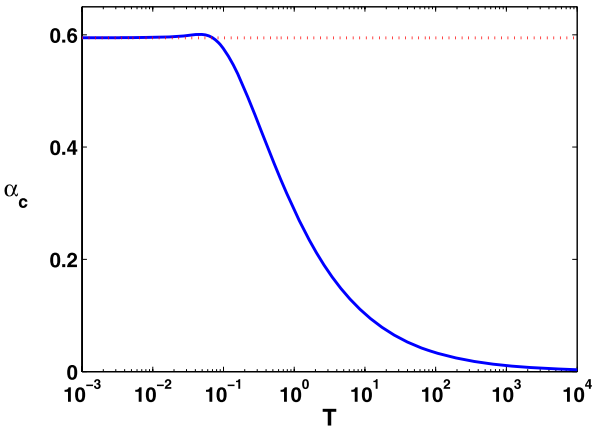

Fig. 4 The critical exponent α_c versus temperature for a particle in a double well potential. α_c marks the transition between a local minimum to a local maximum of the PDF of $\overline{x}$ on $\overline{x}=0$. When $\alpha \to 0$, $f_\alpha(\overline{x}) = p^{\rm eq}(\overline{x})$ and this density has a single peak on $\overline{x}=0$, when $T \to \infty$. It follows that $\alpha_c \to 0$ when $T \to \infty$. Namely the particle does not "notice" the two wells when the temperature is high. When $T \to 0$ we have $\alpha_c \simeq 0.595$

5 From Continuous Time Random Walk to Weak Ergodicity Breaking

In this section we derive our main results using the CTRW approach. To reach (13) we assumed the following: (i) the PDF of the occupation time t_j is the one sided Lévy PDF (3), and (ii) that the total measurement time $t = \sum_{j=1}^{L} t_j$ is a random variable. In Physical experiments the measurement time is fixed. These assumptions are relaxed now using two types of CTRW models. Thermal CTRWs describe a Physical situation where the particle is undergoing a random walk in contact with a thermal heat bath. In this case the equilibrium distribution of an ensemble of particles is Boltzmann's distribution. The second case describes a system far from thermal equilibrium, where a non-thermal equilibrium is reached.

We consider a renewal process for a system with L states $j = 1, \ldots, L$. The system starts in a state j, it waits in this state until time $\bar{t}_1$, it then jumps to some other state say state l, it waits in state l until time $\bar{t}_2$ and then makes another jump. The sojourn times between jump events τ are independent identically distributed random variables with a common PDF $\psi(\tau)$. Our focus is on the case where $\psi(\tau)$ has a long tail $\psi(\tau) \propto \tau^{-(1+\alpha)}$ when $\tau \to \infty$ so $\langle \tau \rangle = \infty$ when $0 < \alpha < 1$. After waiting in a state j a transition to state $l \neq j$ takes place, with probability w_{lj} ($0 \leq w_{lj} \leq 1$, $\sum_{l=1}^{L} w_{lj} = 1$ and $w_{jj} = 0$). We assume that transition probabilities w_{lj} are such that in the limit of long measurement times, all states are visited regardless of the initial condition. In other words, the system is not decomposable into non-accessible regions in the space it samples; where once the system starts in a certain region, it cannot explore all other states. Such a case corresponds to strong ergodicity breaking.

Let N be the random number of jump events (renewals) in the time interval $(0, t)$. Dots on the time axis on which jumps from one state to another occur are denoted with $\bar{t}_i$ and clearly $\bar{t}_N < t < \bar{t}_{N+1}$ namely in the time interval $(0, t)$ $i = 1, \ldots N$. Let n_j be the number of transitions out of state j and clearly $N = \sum_{j=1}^{L} n_j$. Let τ_l^j be the l th sojourn time in state j. And let k be the state of the system at time t. A schematic presentation of the process with three states is shown in Fig. 5. Statistics of the number of renewals N in $(0, t)$ is a well investigated problem [24, 26, 41] for example $\langle N \rangle \sim t^{\alpha}$.

For the CTRW on a one dimensional lattice the states $j = 1, \ldots L$ correspond to the position of the particle on a finite lattice. Then for example the time average of the coordinate of the particle is $\overline{x} = \sum_{j=1}^{L} j t_j / t$ where t_j is the occupation time in state j (see Fig. 5). However, our considerations are more general. For example, for blinking quantum dots [9–12] one state (say $j = 1$) may denote an on state in which many photons are emitted

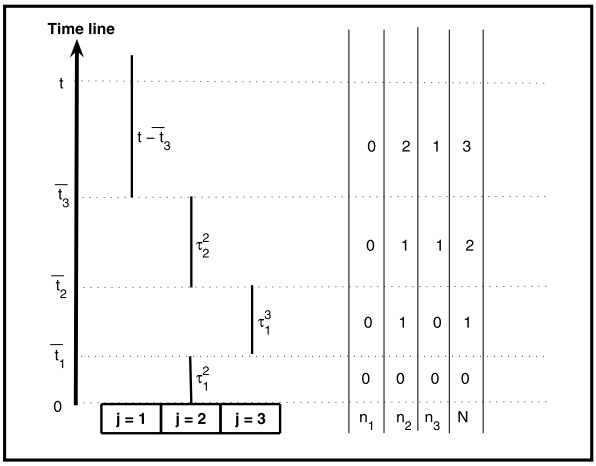

Fig. 5 A schematic diagram of the process for a system with three states, starting in state $j = 2$ and ending in state $j = 1$ (hence k defined in the text is equal 1). In this example the occupation times are $t_1 = t - \bar{t}_3$, $t_2 = (\bar{t}_1 - 0) + (\bar{t}_3 - \bar{t}_2) = \tau_1^2 + \tau_2^2$ and $t_3 = \bar{t}_2 - \bar{t}_1 = \tau_1^3$

and state $j = 2$ is the off state. This system is non-thermal since it is driven by a strong laser field. On the other hand the CTRW dynamics of a probe bead immersed in a polymer actin network [39] is an example for a thermal CTRW motion in a system with a well defined temperature T.

A specific example is the CTRW on a one dimensional lattice with jumps to nearest neighbors only. A particle on j has a probability of jumping left q_j and a probability of jumping right $1 - q_j$ so

$$w_{j-1,j} = q_j \quad \text{and} \quad w_{j+1,j} = 1 - q_j. \tag{46}$$

Reflecting boundary conditions $q_L = 1$ and $q_1 = 0$ are assumed. For $j \neq 1, L$ we must have $q_j \neq 0$ and $q_j \neq 1$ so that all lattice points be visited. Between jumps, the particle waits on a lattice point. The waiting times between the jumps are independent, identically distributed random variables with a common PDF $\psi(\tau)$. This type of random walk leads to anomalous subdiffusion $\langle x^2 \rangle \sim t^\alpha$ when $q_j = 1/2$ and the system is infinite [2, 41].

5.1 Visitation and Population Fractions

The ratio $v_j = n_j/N$ is called the visitation fraction. The population fraction p_j^{eq} is found by considering the ensemble of M non interacting systems. Letting these systems evolve from some initial condition and waiting for the long time limit, $\lim_{M\to\infty} M_j/M = p_j^{\text{eq}}$ where M_j is the number of systems in state j. The population fraction is determined from $w \cdot p^{\text{eq}} = p^{\text{eq}}$.

After many jumps $N \to \infty$ and for any initial condition the visitation fraction reaches an equilibrium and

$$p_j^{\text{eq}} = \lim_{N\to\infty} v_j = v_j^{\text{eq}} \tag{47}$$

so $w \cdot v = v$. To see this note that the visitation fraction is given by $v_j = \sum_{n=1}^{N} \theta_j(n)/N$, where n is a counter of the number of jumps, and $\theta_j(n) = 1$ if the particle is on j after n steps, otherwise it is zero. In the long time limit the PDF of v_j will converge to a narrow distribution centered around its mean so $v_j \simeq \sum_{n=1}^{N} \langle \theta_j(n) \rangle / N$. Let $p_j(n)$ be the probability to be on j after n steps. By definition $\theta_j(n) = 1$ with probability $p_j(n)$ and $\theta_j(n) = 0$ with

probability $1 - p_j(n)$. Hence

$$v_j \simeq \frac{\sum_{n=1}^{N} p_j(n)}{N} \tag{48}$$

or in vector notation $v = (v_1, \ldots, v_L)$, $p(n) = (\ldots, p_j(n) \ldots)$ we have $v \simeq \sum_{n=1}^{N} p(n)/N$. This means that ergodicity holds in discrete time, where the operational time is the number of steps, not the real time. Thus the term *weak* ergodicity breaking [7] is very appealing. Multiplying (48) with w from the left and using $p(n+1) = wp(n)$ we have $w \cdot v \simeq \sum_{n=1}^{N} p(n+1)/N$. Therefore when $N \to \infty$ we have $w \cdot v^{\mathrm{eq}} = v^{\mathrm{eq}}$ which holds in the long time limit. It is important to realize that the visitation fraction and the population fraction are equal since all sojourn times have a common distribution $\psi(\tau)$. We will later consider the more general case where different states may have different waiting time PDFs, and then the visitation fraction is not equal to the population fraction.

5.2 Equilibrium, Thermal Detailed Balance

For the one dimensional CTRW on a lattice the equilibrium population and the visitation fraction are determined from (46)

$$p_j^{\mathrm{eq}} = q_{j+1} p_{j+1}^{\mathrm{eq}} + \left(1 - q_{j-1}\right) p_{j-1}^{\mathrm{eq}}. \tag{49}$$

Using reflecting boundary conditions and (49),

$$p_j^{\mathrm{eq}} = \lim_{N\to\infty} v_j = \frac{1}{1-q_j} \prod_{k=2}^{j} \frac{1-q_k}{q_k} p_1^{\mathrm{eq}}, \tag{50}$$

and from normalization

$$p_1^{\mathrm{eq}} = v_1^{\mathrm{eq}} = \left[1 + \sum_{j=2}^{L} \frac{1}{1-q_j} \prod_{k=2}^{j} \frac{1-q_k}{q_k} \right]^{-1}. \tag{51}$$

When the particle undergoing the CTRW process is coupled to a thermal heat bath, we apply usual detailed balance condition on the transition probabilities [15]. In this case, the visitation fraction will be described by Boltzmann statistics. For example, if q_j is a constant $q > 1/2$ the random walk is biased, which physically corresponds to an external force field $F < 0$, driving the particles to the left. Using lattice spacing a and letting the system be semi-infinite $L \to \infty$, thermal detailed balance condition gives the ratio between the probability of jumping left from point j and the probability of jumping right from point $j-1$:

$$\frac{q_j}{1-q_{j-1}} = \frac{q}{1-q} = \exp\left(\frac{|F|a}{T}\right). \tag{52}$$

Using (47), (50), (51), (52), Boltzmann's statistics hold both for the visitation and the population fractions:

$$\lim_{N\to\infty} v_j = p_j^{\mathrm{eq}} = \frac{\exp\left(-\frac{E_j}{T}\right)}{Z}, \tag{53}$$

for $j > 1$ where $E_j = |F|aj$ is the potential energy, Z is a normalization and for the reflecting boundary $p_1^{\rm eq} = [1 - \exp(-|F|a/T)]/2$. More general thermal detailed balance conditions [15] show that (53) is valid for binding force fields and not limited to the case F being a constant.

5.3 Distribution of Time Averages

The time average of a physical observable is as before

$$\overline{\mathcal{O}} = \frac{\sum_{j=1}^{L} \mathcal{O}_j t_j}{t}, \tag{54}$$

where now the measurement time t is fixed and $\sum_{j=1}^{L} t_j = t$. Let $\vec{\mathcal{O}} = \{\mathcal{O}_1, \ldots \mathcal{O}_L\}$. We consider the moment generating function,

$$\hat{f}_{t,\vec{\mathcal{O}}}(u) = \left\langle \exp\left(-u \sum_{j=1}^{L} \mathcal{O}_j t_j \right) \right\rangle, \tag{55}$$

and in double Laplace space

$$\hat{f}_{s,\vec{\mathcal{O}}}(u) = \int_0^\infty e^{-st} \left\langle \exp\left(-u \sum_{j=1}^{L} \mathcal{O}_j t_j \right) \right\rangle {\rm d}t, \tag{56}$$

so s, t and $u, \sum_{j=1}^{L} \mathcal{O}_j t_j$ are two Laplace pairs. Let $\vec{n} = \{n_1, \ldots, n_L\}$. We consider the generating function conditioned that the system made N transitions and $\vec{n}$ describes the number of renewals in each state. The occupation time in state $j \neq k$ is

$$t_j = \sum_{l=1}^{n_j} \tau_l^j \tag{57}$$

and for state k (recall this is the state of the system at time t)

$$t_k = t - \bar{t}_N + \sum_{l=1}^{n_k} \tau_l^k. \tag{58}$$

The time $t - \bar{t}_N$ is called the backward recurrence time, it is the time between the last jump event in $(0, t)$ and the measurement time t. Using (57), (58), the conditioned generating function is

$$\hat{f}_{s,\vec{\mathcal{O}},N,\vec{n}}(u) = \left\langle \int_0^\infty {\rm d}t \exp\left[-st - u\mathcal{O}_k \left(t - \bar{t}_N + \sum_{l=1}^{n_k} \tau_l^k \right) - \sum_{j=1, j\neq k}^{L} u\mathcal{O}_j \sum_{l=1}^{n_j} \tau_l^j \right] \right.$$
$$\left. \times\, I\left(\bar{t}_N < t < \bar{t}_{N+1} \right) \right\rangle, \tag{59}$$

where $I(x) = 1$ if the condition in the parenthesis is true, otherwise $I(x) = 0$. First we integrate over t and obtain

$$\hat{f}_{s,\vec{\mathcal{O}},N,\vec{n}}(u) = \left\langle \frac{e^{-s\bar{t}_N} - e^{-s\bar{t}_{N+1} - u\mathcal{O}_k(\bar{t}_{N+1} - \bar{t}_N)}}{s + u\mathcal{O}_k} e^{-\sum_{j=1}^{L} u\mathcal{O}_j \sum_{l=1}^{n_j} \tau_l^j} \right\rangle, \tag{60}$$

then we use the assumption of independent and identically distributed sojourn times τ, and the identities $\bar{t}_N = \sum_{j=1}^{L} \sum_{l=1}^{n_j} \tau_j^l$, $\bar{t}_{N+1} = \bar{t}_N + \tau_k^{n_k+1}$ to find

$$\hat{f}_{s,\vec{\mathcal{O}},N,\vec{n}}(u) = \frac{\prod_{j=1}^{L} \hat{\psi}^{n_j}\left(s+u\mathcal{O}_j\right)\left[1-\hat{\psi}\left(s+u\mathcal{O}_k\right)\right]}{s+u\mathcal{O}_k}, \tag{61}$$

where $\hat{\psi}(s) = \int_0^\infty \psi(\tau)\exp(-s\tau)\mathrm{d}\tau$ is the Laplace transform of $\psi(\tau)$.

In the limit of long measurement time, corresponding to the usual small s and u limit, their ratio being finite, the system will reach an equilibrium for the number of renewals in each state. Namely from (47), the visitation fraction will satisfy

$$v_j^{\mathrm{eq}} = \lim_{N\to\infty} \frac{n_j}{N} = p_j^{\mathrm{eq}}. \tag{62}$$

We use (62) in (61), then insert the usual small s behavior [5, 24, 26, 41]

$$\hat{\psi}(s) \sim 1 - As^{\alpha}, \tag{63}$$

which corresponds to $\psi(\tau) \sim A\tau^{-(1+\alpha)}/|\Gamma(-\alpha)|$ and find

$$\hat{f}_{s,\vec{\mathcal{O}},k}(u) \sim \frac{\left(s+u\mathcal{O}_k\right)^{\alpha-1}}{\sum_{j=1}^{L} p_j^{\mathrm{eq}}\left(s+u\mathcal{O}_j\right)^{\alpha}}. \tag{64}$$

Summing over all final states k, with the final weights, we find

$$\hat{f}_{s,\vec{\mathcal{O}}}(u) \sim \frac{\sum_{j=1}^{L} p_j^{\mathrm{eq}}\left(s+u\mathcal{O}_j\right)^{\alpha-1}}{\sum_{j=1}^{L} p_j^{\mathrm{eq}}\left(s+u\mathcal{O}_j\right)^{\alpha}}. \tag{65}$$

Using a method found in the Appendix of Ref. [26], we invert (65) and find our main result (13).

5.4 Numerical Examples

To demonstrate our results we consider an unbiased CTRW. We consider a model with $L = 30$ sites on $j = 1, \ldots 30$ jumps are to nearest neighbors only with $q_j = 1/2$ with periodic boundary conditions. We used the waiting time PDF $\psi(\tau) = \alpha\tau^{-\alpha-1}$ for $\tau > 1$ otherwise $\psi(\tau) = 0$. The observable is x, the position of the particle, which attains the values $x = 1, \ldots, j, \ldots, 30$. Simulating trajectories of a single particle we calculate the time average $\overline{x} = \sum_{j=1}^{30} jt_j/t$ and then repeat the experiment many times and construct the distribution of $\overline{x}$.

In Figs. 6, 7 we show single particle trajectories and their time average for $\alpha = 0.3$ and $\alpha = 0.75$, respectively. The time average is clearly a fluctuating random variable, due to long sticking times in states of the system. Notice that the particle visits all lattice points, and the phase space is not decomposable into inaccessible regions as found for strong ergodicity breaking. For a waiting time PDF $\psi(\tau) = 5\tau^{-6}$ for $\tau > 1$, we have a finite average waiting time, and hence as shown in Fig. 8 we find an ergodic behavior $\overline{x} \simeq \langle x\rangle = (L+1)/2 = 15.5$ in the long time limit.

In Figs. 9, 10 we present the PDF of $\overline{x}$ for $\alpha = 0.75$ and $\alpha = 0.3$, respectively. Comparison between simulations and theory (13) show excellent agreement without fitting. In (13)

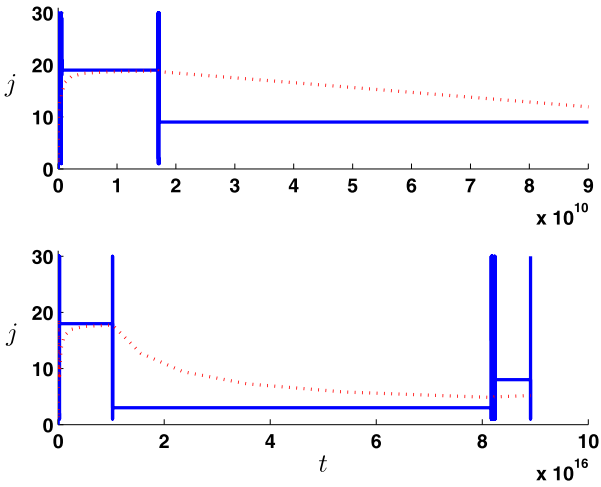

Fig. 6 Trajectory of a single CTRW particle on a lattice, with $\alpha = 0.3$ (*solid curve*, *blue online*). Long waiting times, of the order of the measurement time dominate the landscape. The time average $\overline{x}$ is a random variable (*dotted curve*, *red online*)

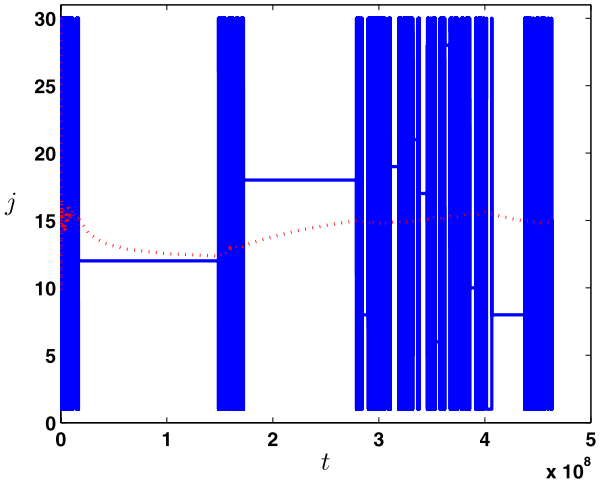

Fig. 7 Same type of non-ergodic behavior as found in Fig. 6 however now $\alpha = 0.75$

we use $p_j^{\rm eq} = 1/L$, which is the obvious population probability. The number of realizations was 120000 and the simulation time $t = 10^8, 10^{12}$ for Figs. 9, 10 respectively. In Figs. 9, 10 we also show the continuum approximation (43). From Figs. 9, 10 we see that the structure of the lattice is encoded in the distribution of the time average $\overline{x}$. Since the observable at any given moment of time attains the values $x = 1, \ldots 30$ we have 30 divergences in Figs. 9, 10 in agreement with the more general rule discussed under (16). When the system is made large, these effects become negligible and the continuum approximation works well.

5.5 Non Identical Waiting Time Distributions

The CTRW considers a situation where a single waiting time PDF $\psi(\tau)$ describes the dynamics. What happens when the waiting times in the states j are not identically distributed? For example, consider the aforementioned blinking quantum dots [9–12]. The quantum dot when interacting with a laser field will switch between an on state (+) where many photons

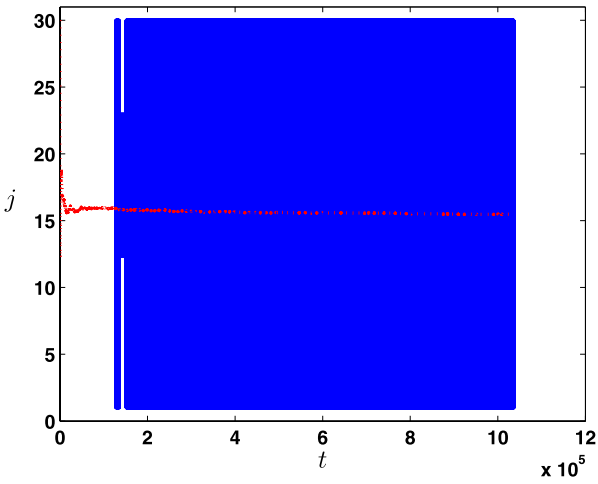

Fig. 8 Same as Fig. 6, however now $\psi(\tau) = 5\tau^{-6}$ for $\tau > 1$. After a short transient the time average (the *dotted curve*) converges to the ensemble average on 15.5 indicating ergodicity

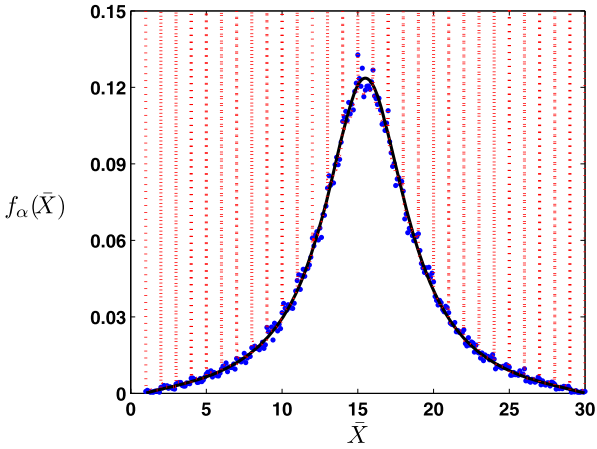

Fig. 9 Distribution of the time average $\overline{x}$ for $\alpha = 3/4$. Numerical simulations of the CTRW process on a lattice (*dots*) are well approximated with the continuum limit (43) (*solid curve*). The dotted curve with divergences on the lattice points is the analytical theory (13)

are emitted and an off $(-)$ state. The sojourn times in state on (and off) are independent identically distributed random variables [42]. The PDF of sojourn times in states on and off follow power law statistics at least within a long experiment time [12], and in Laplace space $\hat{\psi}_{\pm}(s) \sim 1 - A_{\pm}s^{\alpha} + \cdots$. This two state renewal process is characterized with two amplitudes A_+ and A_-, and in this sense it differs from the usual CTRW. It is worthwhile to note that the visitation fraction in states $\pm$ clearly satisfy

$$\lim_{N\to\infty} v_{\pm} = \lim_{N\to\infty} \frac{n_+}{N} = \lim_{N\to\infty} \frac{n_-}{N} = \frac{1}{2} \tag{66}$$

in the limit of long measurement time, where N is the total number of transitions between states on and off. If we consider an ensemble of M independent blinking dots, the population fraction of the number of dots in state on $(+)$ M_+ and off $(-)$ M_- is

$$p_{\pm}^{\mathrm{eq}} = \lim_{M\to\infty} \frac{M_{\pm}}{M} = \frac{A_{\pm}}{A_- + A_+}, \tag{67}$$

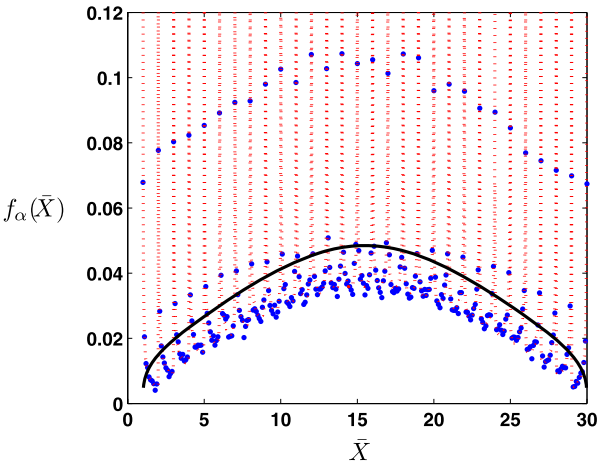

Fig. 10 Same as Fig. 9 for $\alpha = 0.3$. Now the fluctuations are larger compared with the $\alpha = 3/4$ case and the underlying structure of the lattice is more important. Of course bin size must be made small enough for the lattice effect to be observed

where the population fraction is measured in the limit of long measurement time. So here the visitation fraction and the population fraction are non-identical if $A_+ \neq A_-$.

More generally, we consider the renewal dynamics with power law waiting times in each state. However, now

$$\hat{\psi}_j(s) \sim 1 - A_j s^\alpha \tag{68}$$

when the Laplace variable $s \to 0$, $A_j > 0$ for $j = 1, \ldots, L$ and $0 < \alpha < 1$. In this case the population fractions are related to the visitation fractions according to

$$p_j^{\rm eq} = \lim_{N\to\infty} \frac{A_j v_j^{\rm eq}}{\sum_{i=1}^L A_i v_i^{\rm eq}} \tag{69}$$

and $w \cdot v = v$. Now the main equations derived in this section must be modified, for example (61)

$$\hat{f}_{s,\vec{\mathcal{O}},N,\vec{n}}(u) = \frac{\prod_{j=1}^L \hat{\psi}_j^{n_j}\left(s + u\mathcal{O}_j\right)\left[1 - \hat{\psi}_k\left(s + u\mathcal{O}_k\right)\right]}{s + u\mathcal{O}_k}. \tag{70}$$

Then using (68)–(70), we find (13) (the method is nearly identical to the case where all the waiting times are identical). Thus while the dynamics clearly differ from the usual CTRW with a single waiting time PDF, and the visitation fraction is not identical to the population fraction, our main result for the distribution of the time averages equation (13) is still valid.

Another situation occurs when the system has different types of waiting times, for example some states may have exponential waiting times while others follow power law statistics. Or we may have some states with a power law waiting time PDF with an exponent $0 < \alpha_1 < 1$ and for other states an exponent $0 < \alpha_2 < \alpha_1$. Also in this case, our main result (13) will be valid. In the long time limit the system will occupy only the states with the smallest $\alpha < 1$. Only those states are relevant for the calculation of the distribution of time averages (13). Other states might be visited many times so their visitation fraction is not necessarily small. However the time spent by the system in these states is negligible and they do not contribute to the time average.

6 Discussion

For Boltzmann–Gibbs statistical mechanics it is assumed that occupation fractions are identical to the population fractions, and thus time averages and ensemble averages are identical. Ergodicity can be broken when the system is decomposable into several regions of its phase space, in such a way that once the system starts in one region it cannot explore other parts of the system. In this case, time averages depend on the initial condition of the system. In contrast, in weak ergodicity breaking, the divergence of the average sojourn times, leads to ergodicity breaking. Unlike decomposable systems, for dynamics described by power law distribution of waiting times, the entire phase space is explored. This has strong consequences that are encoded in our main equation (13) for the distribution of the time average. This equation shows that the equilibrium populations describing an ensemble of systems i.e. $p_j^{\rm eq}$, enter in the distribution of the time averaged observables. Hence in this sense we can construct a non-ergodic statistical theory, that is not specific to a particular initial condition, and which relates distributions of time averages with populations of ensembles.

Acknowledgements This work was supported by the Israel Science Foundation. E.B. thanks G. Margolin, S. Burov, and G. Bel for discussions.

References

1. Van Kampen, N.G.: Stochastic Processes in Physics and Chemistry. North Holland, Amsterdam (1992)
2. Scher, H., Montroll, E.W.: Phys. Rev. B **12**, 2455 (1975)
3. Bouchaud, J.P., Georges, A.: Phys. Rep. **195**, 127 (1990)
4. Klafter, J., Shlesinger, M.F., Zumofen, G.: Phys. Today **49**, 33 (1996)
5. Metzler, R., Klafter, J.: Phys. Rep. **339**, 1 (2000)
6. Klages, R., Radons, G., Sokolov, I.M. (eds.): Anomalous Transport Foundations and Applications. Wiley-VCH, Weinheim (2008)
7. Bouchaud, J.P.: J. De Phys. I **2**, 1705 (1992)
8. Aaronson, J.: An Introduction to Infinite Ergodic Theory. Mathematical Surveys and Monographs American Mathematical Society, Providence (1997)
9. Brokmann, X., Hermier, J.-P., Messin, G., Desbiolles, P., Bouchaud, J.-P., Dahan, M.: Phys. Rev. Lett. **90**, 120601 (2003)
10. Margolin, G., Barkai, E.: Phys. Rev. Lett. **94**, 080601 (2005)
11. Margolin, G., Protasenko, V., Kuno, M., Barkai, E.: Adv. Chem. Phys. **133**, 327 (2006)
12. Margolin, G., Protasenko, V., Kuno, M., Barkai, E.: J. Phys. Chem. B **110**, 19053 (2006)
13. Margolin, G., Barkai, E.: J. Stat. Phys. **122**, 137 (2006)
14. Bel, G., Barkai, E.: Phys. Rev. Lett. **94**, 240602 (2005)
15. Bel, G., Barkai, E.: Phys. Rev. E **73**, 016125 (2006)
16. Barkai, E.: J. Stat. Phys. **123**, 883 (2006)
17. Thaler, M.: Ergo. Th. & Dynam. Syst. **22**, 1289 (2002)
18. Bel, G., Barkai, E.: Europhys. Lett. **74**, 15 (2006)
19. Akimoto, T.: J. Stat. Phys. **132**, 171 (2008)
20. Heinsalu, E., Patriarca, M., Goychuk, I., Schmid, G., Hanggi, P.: Phys. Rev. E **73**, 046133 (2006)
21. Lomholt, M.A., Zaid, I.M., Metzler, R.: Phys. Rev. Lett. **98**, 200603 (2007)
22. Burov, S., Barkai, E.: Phys. Rev. Lett. **98**, 250601 (2007)
23. Rebenshtok, A., Barkai, E.: Phys. Rev. Lett. **99**, 210601 (2007)
24. Feller, W.: An Introduction to Probability Theory and its Applications. Wiley, New York (1970)
25. Redner, S.: A Guide to First-Passage Processes. Cambridge University Press, Cambridge (2001)
26. Godreche, C., Luck, J.M.: J. Stat. Phys. **104**, 489 (2001)
27. Lamperti, J.: Trans. Am. Math. Soc. **88**, 380 (1958)
28. Barlow, M.T., Pitman, J., Yor, M.: Sémin. de Probab. de Strasb. **23**, 294 (1989)
29. Samorodnitsky, G., Taqqu, M.S.: Stable Non-Gaussian Random Processes. Chapman & Hall/CRC, London (2000)
30. Barkai, E.: Phys. Rev. E **63**, 046118 (2001)

31. Metzler, R., Barkai, E., Klafter, J.: Phys. Rev. Lett. **82**, 3563 (1999)
32. Barkai, E., Metzler, R., Klafter, J.: Phys. Rev. E **61**, 132 (2000)
33. Gorenflo, R., Mainardi, F., Vivoli, A.: Chaos, Solitons Fractals **34**, 87 (2007)
34. Kleinhans, D., Friedrich, R.: Phys. Rev. E **76**, 061102 (2007)
35. Eule, S., Friedrich, R., Jenko, F., Kleinhans, D.: J. Phys. Chem. B **111**, 11474 (2007)
36. Magdziarz, M., Weron, A., Weron, K.: Phys. Rev. E **75**, 016708 (2007)
37. Zumofen, G., Klafter, J.: Phys. Rev. E **47**, 851 (1993)
38. Baldassarri, A., Bouchaud, J.P., Dornic, I., Godreche, C.: Phys. Rev. E **59**, R20 (1999)
39. Wong, I.Y., Gardel, M.L., Reichman, D.R., Weeks, E.R., Valentine, M.T., Bausch, A.R., Weitz, D.A.: Phys. Rev. Lett. **92**, 178101 (2004)
40. Golding, I., Cox, E.C.: Phys. Rev. Lett. **96**, 098102 (2006)
41. Shlesinger, M.F.: J. Stat. Phys. **10**, 421 (1974)
42. Bianco, S., Grigolini, P., Paradisi, P.: J. Chem. Phys. **123**, 174704 (2005)